REVIEW ARTICLE
Cytoskeleton, October 2012 69:738–750 (doi: 10.1002/cm.21050)

Growth, Interaction, and Positioning of Microtubule Asters in Extremely Large Vertebrate Embryo Cells

Timothy Mitchison, Martin Wühr, Phuong Nguyen, Keisuke Ishihara, Aaron Groen, and Christine M. Field*

Department of Systems Biology, Harvard Medical School and Marine Biological Laboratory, Woods Hole, Massachusetts

Received 1 April 2012; Revised 27 June 2012; Accepted 28 June 2012
Monitoring Editor: Douglas Robinson

Ray Rappaport spent many years studying microtubule asters, and how they induce cleavage furrows. Here, we review recent progress on aster structure and dynamics in zygotes and early blastomeres of *Xenopus laevis* and Zebrafish, where cells are extremely large. Mitotic and interphase asters differ markedly in size, and only interphase asters span the cell. Growth of interphase asters occurs by a mechanism that allows microtubule density at the aster periphery to remain approximately constant as radius increases. We discuss models for aster growth, and favor a branching nucleation process. Neighboring asters that grow into each other interact to block further growth at the shared boundary. We compare the morphology of interaction zones formed between pairs of asters that grow out from the poles of the same mitotic spindle (sister asters) and between pairs not related by mitosis (non-sister asters) that meet following polyspermic fertilization. We argue growing asters recognize each other by interaction between antiparallel microtubules at the mutual boundary, and discuss models for molecular organization of interaction zones. Finally, we discuss models for how asters, and the centrosomes within them, are positioned by dynein-mediated pulling forces so as to generate stereotyped cleavage patterns. Studying these problems in extremely large cells is starting to reveal how general principles of cell organization scale with cell size. © 2012 Wiley Periodicals, Inc

Key Words: aster, embryo, microtubule, cleavage, centrosome

*Address correspondence to: Christine M. Field, Department of Systems Biology, Harvard Medical School and Marine Biological Laboratory, Woods Hole, Massachusetts.
E-mail: christine_field@hms.harvard.edu

Published online 20 August 2012 in Wiley Online Library (wileyonlinelibrary.com).

Introduction

Microtubule asters—radial arrays of microtubules radiating from centrosomes—play a central organizing role in early embryos. Ray Rappaport was fascinated by the question of how asters, in particular pairs of asters, induce cleavage furrows. One of his most celebrated discoveries [Rappaport, 1961] was that neighboring pairs of microtubule asters can induce cleavage furrows in echinoderm embryos whether the asters arise from the poles of the same mitotic spindle (which we will call sisters) or from juxtaposed poles of two different spindles (which we will call non-sisters). This discovery had a profound influence on subsequent thinking in the cytokinesis field. How microtubules communicate with the cortex is the subject of other articles in this volume. Here, we will take a more microtubule-centric perspective, and ask: how do asters grow, how do they interact with other asters, and how are they positioned in the cytoplasm? These processes determine where aster pairs will interact with the cortex, and thus define cleavage plane geometry. We will discuss how these processes occur in zygotes and early blastomeres of amphibians and Zebrafish, which provide convenient experimental systems, but also represent extremely large cells. Comparison with similar processes in smaller cells will reveal how conserved, microtubules-based spatial organizing mechanisms scale with cell size.

The amphibian *Xenopus laevis* and the fish *Danio rerio* (Zebrafish) are easy to rear in the laboratory, and offer complementary technical advantages. *Xenopus* eggs cleave completely and are easy to fertilize with one or multiple sperm and to microinject. They are opaque, which precludes live imaging of internal events, but fixed embryos can be cleared for immunofluorescence imaging by immersion in a high refractive index medium [Klymkowsky and Hanken, 1991; Becker and Gard, 2006]. Importantly for us, essentially undiluted cell-free extracts can be prepared from *Xenopus* eggs which recapitulate much of the biology of the early embryo and are highly tractable for biochemical manipulation, physical manipulation, and

live imaging [Desai et al., 1999; Chan and Forbes, 2006; Maresca and Heald, 2006]. Early Zebrafish embryos are meroblastic, that is, they do not cleave completely. Their animal pole region is yolk-free and transparent, which allows live imaging. Zebrafish are highly tractable for classic genetics, and transgenic lines that stably express green fluorescent protein (GFP)-tagged proteins can be generated easily. The mechanisms we discuss are broadly conserved in evolution, and important comparison systems with smaller cells include embryos of marine invertebrates, *C. elegans* and *Drosophila* as well as somatic cells. *Drosophila* offers an interesting biological twist in that early divisions are syncytial, so aster growth and interactions are uncoupled from cytokinesis for the first 12 cell cycles.

Xenopus and Zebrafish zygotes and early blastomeres are extremely large cells, with zygotes ~1200 μm and ~600 μm in diameter, respectively. They are also unusually fast compared to somatic cells, in the sense that the cell cycle takes 20–30 min to complete at room temperature (the first cell cycles are longer). These sizes and speeds represent physical extremes compared to typical somatic cells, which may require special adaptations of conserved cell organizing mechanisms, and/or reveal underappreciated intrinsic capabilities of those mechanisms. One well-studied example is adaptation of replication origins for very fast genome duplication [Blow, 2001]. Here, we will focus on adaptations of aster growth and interaction mechanisms that allow rapid and accurate spatial organization on a scale of hundreds of μm. This is much larger than the molecular length scale, and may even be larger than the microtubule length scale inside the aster.

Aster Growth in Large Cells

The question of how microtubule asters grow in extremely large embryo cells has received little attention, but we believe that answering it will reveal principles of size scaling and unexpected molecular mechanisms. Figures 1 and 2 illustrate aster morphology and growth during the first and second cell cycle in frog and fish embryos. Inspection of these and similar images [Wühr et al., 2009, 2010, 2011] suggests that the structure of large interphase asters in these embryos does not conform to the standard model, where all microtubules radiate as straight lines from a single point at the centrosome. Rather, the microtubule network in the asters appears bushy and single microtubules or thin bundles at the aster periphery appear wavy or curved (Fig. 2 last panel). Least consistent with the conventional model, microtubule density at the aster periphery appears to remain constant, or increase, with aster radius (Fig. 1) and time (Fig. 2). These images forced us to reconsider the standard model for aster growth, and how it scales with cell size.

Figure 3A illustrates the standard model for aster growth, which we call the radial elongation model. Centrosomes nucleate microtubules and hold on to minus ends, while plus ends elongate in a liner trajectory by addition of GTP-tubulin. This mechanism was inferred from analysis of nucleation and elongation in cultured mammalian cells and isolated centrosomes [Bergen et al., 1980; Brinkley et al., 1981; Brinkley, 1985]. It remains the standard model for animal cells, though many instances are known where microtubules nucleate from locations other than centrosomes [reviewed in Lüders and Stearns, 2007]. We believe there is a fundamental problem in scaling the radial elongation model to large cells. Microtubule density at the periphery must decrease with aster radius in this model. In extremely large cells, the density of microtubules at the periphery would become so low that signaling to the cortex to initiate cytokinesis might become impossible. This problem could be solved, theoretically, by increasing centrosome size. Centrosome size does indeed scale with cell size in *C. elegans* embryos [Decker et al., 2011], and centrosomes in marine invertebrate embryos can be many microns in diameter in the first cell cycle (Fig. 4) [Asnes and Schroeder, 1979; Strickland et al., 2004; Foe and von Dassow, 2008]. It is difficult to precisely define interphase centrosome size in images of early frog and fish embryos. However, by both microtubule (Figs. 1 and 2) and γ-tubulin staining (Fig. 1D′) centrosomes appear small compared to cell size, suggesting there may be an upper limit to centrosome size, as there is to spindle length [Wühr et al., 2008]. It thus appears that the problem of scaling aster size to cell size in very large cells is not solved by scaling centrosome size. Figures 3B–3D illustrate various candidate additions or alternatives to the radial elongation model to solve the size scaling problem and account for observed aster morphology. Whatever the molecules involved, the mechanism by which a growing aster adds new microtubules as it's radius increases must generate an approximately constant density at the periphery, with plus ends pointing on average outward.

Figure 3B illustrates a model in which microtubules are nucleated within the aster as it grows, but away from the centrosome. Nucleation could occur from the side of existing microtubules like Arp2/3 nucleation of actin [Pollard and Borisy, 2003], from Golgi membranes within the aster [Efimov et al., 2007; Rivero et al., 2009], or from some other location. We currently favor this class of model based on morphology and precedent from other systems. Microtubule nucleation from the sides of preexisting microtubules has been observed in several systems, including the cortex of higher plant cells [Murata et al., 2005; Chan et al., 2009; Kirik et al., 2012], and in cytoplasmic bundles in *S. pombe* [Samejima et al., 2006]. In both cases, γ-tubulin complex is recruited to the side of preexisting microtubules where it nucleates and holds on to a new minus end. The regulators are best characterized in *S. pombe*, where the Mto1.Mto2 complex recruits

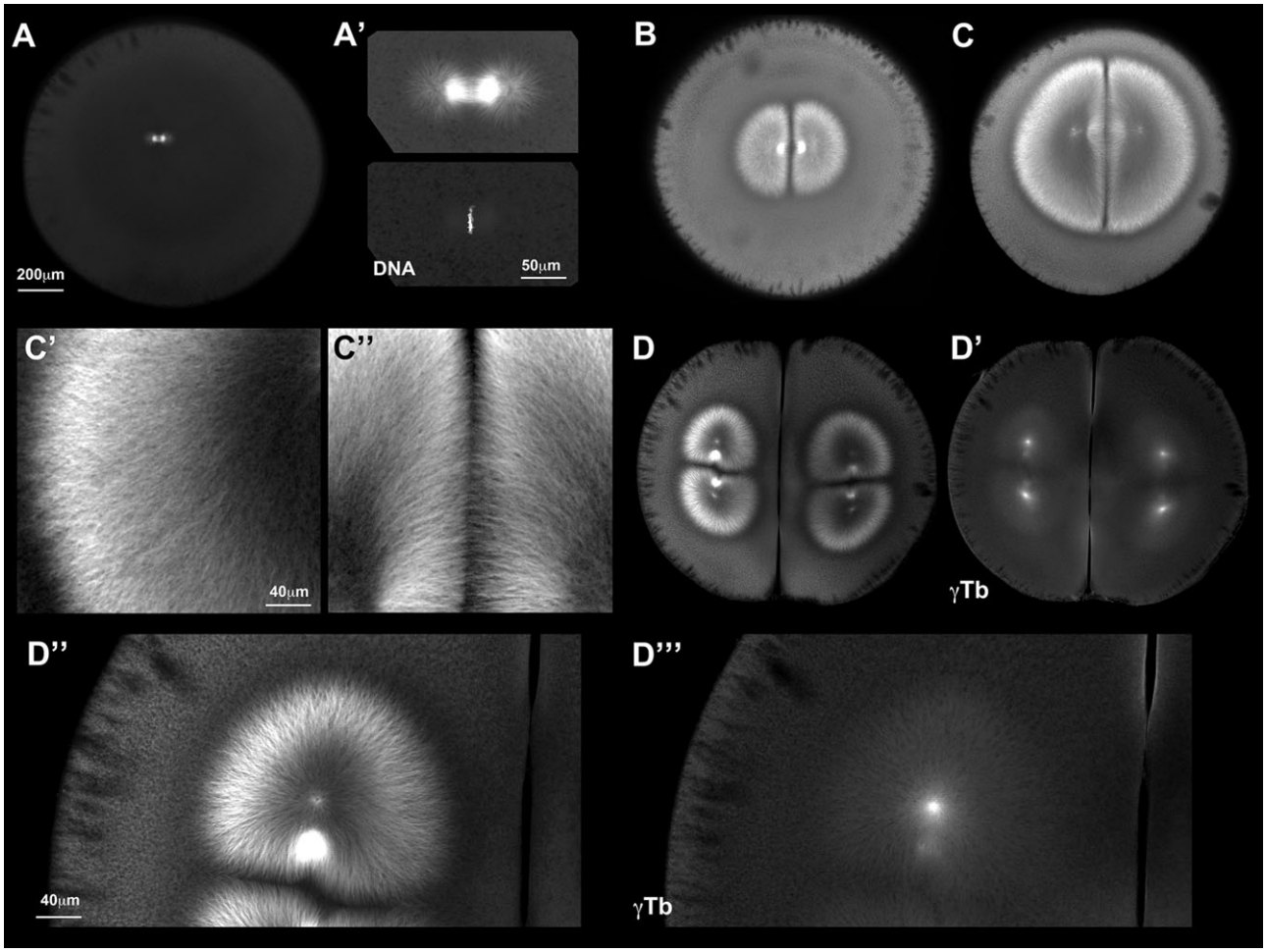

Fig. 1. Growth and interaction of sister asters in the first two divisions in *X. laevis*. Fertilized eggs were fixed, stained for tubulin (**A**, A′ upper, **B, C,** C′, C″, **D**, D″) DNA (A′ lower) and γ-tubulin (D′,D‴) as described [Wühr et al., 2010]. The animal half of the egg was cut off and imaged from the cut surface, so the *z*-axis is parallel to the animal-vegetal axis of the zygote. One letter is used to designate each different embryo. A, A′: metaphase of first mitosis. Note small asters. B: anaphase–telophase of first mitosis. Note aster growth and formation of an interaction zone between sister asters at mid-cell. C, C′, C″: later telophase. Note the dense, bushy appearance of microtubules at the aster periphery, low microtubule density, and probable antiparallel bundles in the interaction zone. D, D′, D″, D‴ telophase of 2nd mitosis, with the 1st cleavage plane oriented North-South. The presumptive 2nd cleavage plane will cut each blastomere between sister asters, at ∼90° to the 1st cleavage plane. Note bushy asters and interaction zones. γ-tubulin staining is brightest at points corresponding to centrosomes, but dimmer staining is evident throughout the aster.

γ-tubulin to the side of preexisting microtubules, and activates it to nucleate [Samejima et al., 2006]. A similar function was proposed for the Augmin/Haus complex in the mitotic spindle and cytokinesis midzone complex of animal cells [Uehara et al., 2009]. Structural studies of γ-tubulin ring complexes predict that the complex needs to undergo a conformational change to become active in nucleation [Kollman et al., 2011]. Microtubule nucleation is, in general, poorly understood at a biophysical level, and pure proteins reconstitution studies are needed to elucidate the mechanisms by which γ-tubulin is recruited and activated in any system. A recent study showed that a centrosomal γ-tubulin recruitment factor, CDK5RAP2, could stimulate nucleation by isolated γ-tubulin complexes [Choi et al., 2010], an encouraging step toward full reconstitution. In favorable immunofluorescence images, we observe a diffuse glow of γ-tubulin in large asters in *Xenopus* embryos (Fig. 1D′), but its significance is unclear.

Figure 3C illustrates a model in which microtubules continually release from the centrosome and slide outward. This mechanism was posited to account for non-centrosomal microtubules in neurons [Ahmad and Baas, 1995], and astral microtubules have been shown to detach and slide outward during anaphase–telophase in tissue culture cells [Rusan et al., 2002]. We know that dynein exerts outward pulling force on astral microtubules during anaphase–telophase in early embryos (discussed below). The same force might well cause outward microtubule sliding, so this model is plausible.

Figure 3D illustrates a model in which the growing aster captures microtubules that were nucleated outside the aster, for example, by the cortex or distributed organelles.

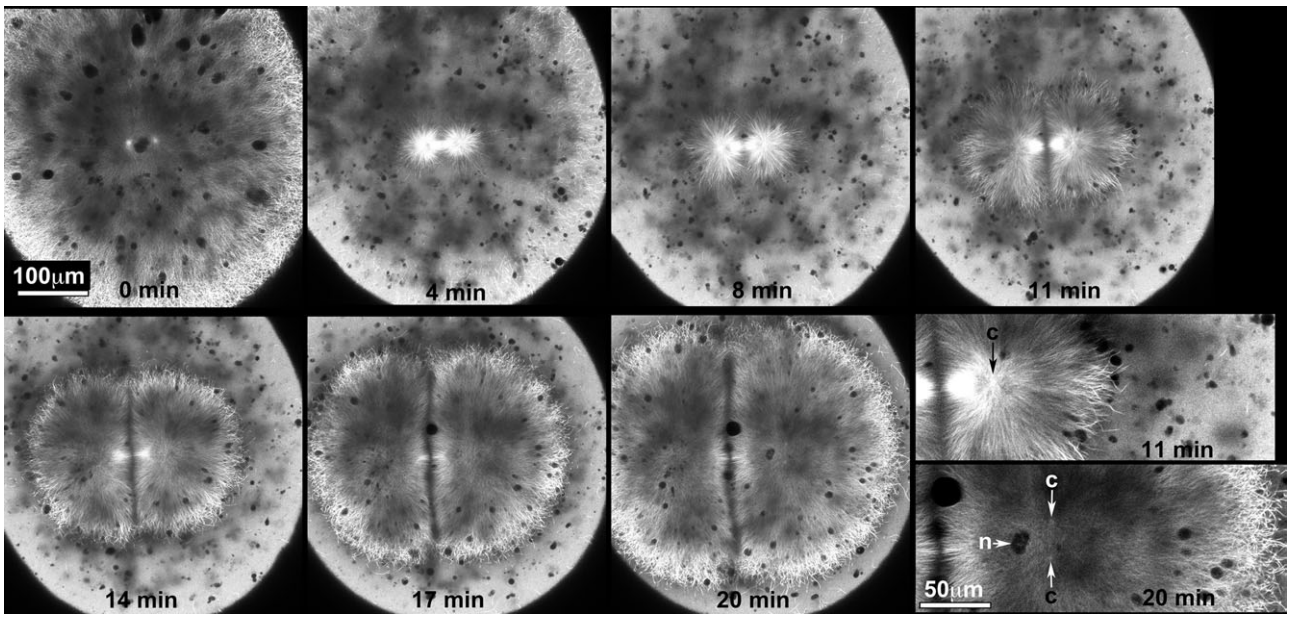

Fig. 2. Growth and interaction of sister asters in Zebrafish 1st mitosis. Fertilized eggs from fish stably expressing the microtubule binding domain of ensconsin fused to 3×GFP were imaged live by confocal microscopy [Wühr et al., 2010, 2011]. The cell is imaged with the animal pole next to the ×20 immersion objective lens. 0 min: prophase, note the intact nucleus. 4 min: metaphase, note the small aster radius at this stage. 8–20 min: after anaphase onset, the paired sister asters rapidly grow, and they meet and interact at the midplane of the cell. Note that the density of microtubules at the aster periphery, which is artificially highlighted using the ensconsin probe, remains approximately constant. Note also that microtubules at the aster periphery often appear curved and somewhat disorganized. The nucleus (n) and centrosomes (c) are highlighted in the last panel. Note the centrosomes inside one aster separate on the north–south axis as they move away from the interaction zones. The 2nd mitotic spindles will later assemble on this north–south axis.

Possibly consistent with this model, prometaphase asters in tissue culture cells capture and orient non-centrosomal microtubules using dynein [Rusan et al., 2002], though this activity probably requires a mitotic state of the cytoplasm where dynein acts to cluster minus ends [Gatlin et al., 2009]. We currently disfavor this model as a major aster growth mechanism in early frog and fish embryos because we do not observe many microtubules in the cytoplasm between the expanding aster periphery and the cortex, but we cannot rule it out.

An important question is whether the unusual aster growth mechanisms illustrated in Fig. 3 apply in other cells. In echinoderm zygotes (~50–200 μm in diameter), astral microtubules appear radial in metaphase, but more complex in anaphase–telophase [Strickland et al., 2004; Foe and von Dassow, 2008]. In Fig. 4, we show images of microtubules in metaphase and anaphase in zygotes of Cerebratulus, a nemertean ribbon worm with eggs ~100 μm in diameter, kindly provided by George von Dassow (Oregon Institute of Marine Biology). At 1st metaphase, most microtubules appear to radiate from large centrosomes, and the density clearly drops with radius (Fig. 4A). These images are consistent with all microtubule initiating at centrosomes and growing out to the cortex, as has been shown in *C. elegans* embryos by EB1 tracking [Srayko et al., 2005]. At anaphase–telophase, the microtubule distribution appears to change. Microtubule density no longer decreases with radius as strongly, and some degree of bushiness is evident toward the periphery (Fig. 4B). Microtubules also appear more bundled. This kind of image suggests that one or more of the mechanism illustrated in Figs. 3B and 3C may operate at telophase in zygotes that are smaller than *Xenopus* and Zebrafish, but still large compared to somatic cells.

Aster size in frog and fish embryos is temporally controlled by the cell cycle, with important implications for growth mechanisms and embryo organization. Aster radius at the poles of the first metaphase spindle is ~30–40 μm in *Xenopus* [Figs. 1A and 1B, Wühr et al., 2008] and similar in Zebrafish [Fig. 2, 4 min, Wühr et al., 2010]. In both cases, this is much smaller than the zygote radius. Asters grow dramatically at anaphase onset, presumably due to decreased activity of Cdk1 (Cdc2.Cyclin B) kinase. In mitosis, Cdk1 acts on a complex network of microtubule interacting proteins to promote catastrophes (growing to shrinking transitions) and limit length [Belmont et al., 1990; Verde et al., 1992; Niethammer et al., 2007]. Microtubule growth in this regime was termed "bounded," because while the lengths of individual microtubules fluctuate by dynamic instability, the average length does not increase with time [Verde et al., 1992]. Aster radius at metaphase, when Cdk1 activity is high, is

presumably limited by the length distribution of microtubules in this bounded regime. Cdk1 levels drop shortly after fertilization, and at anaphase onset [reviewed in Morgan, 2006]. This lowers the catastrophe rate, and allows microtubules to grow longer. Experiments in *Xenopus* extract suggest growth of individual microtubule may become unbounded in interphase [Verde et al., 1992], so in principle single microtubules might elongate continuously from the centrosome to the cortex, hundreds of μm in early frog and fish embryos. The actual length of individual microtubules in large interphase asters is currently unknown. If microtubules are in fact short compared to aster radius, as is the case for *Xenopus* meiosis-II spindles [Burbank et al., 2006], a serious rethink of aster mechanics will be required.

Cell cycle regulation of aster size has important implications for spatial organization of the early embryo. In early frog or fish blastomeres metaphase spindles are centrally located, and their short astral microtubules do not reach the cortex (Fig. 1B) [Wühr et al., 2009, 2010]. Thus, metaphase spindles cannot position themselves relative to the cell cortex using their astral microtubules as usually proposed. In smaller embryos, such as sea urchin, *C. elegans* and Cerebratulus (Fig. 4A) astral microtubules reach the cortex in metaphase, and metaphase spindle can position themselves. In early divisions in frog and fish, the centrosome pairs that initiate the spindles are prepositioned by astral microtubules during the preceding interphase [Wühr et al., 2010]. Following anaphase onset, asters rapidly grow to span the whole cell, and touch the cortex, by one or more of the mechanisms illustrated in Fig. 3. Touching the cortex is presumably required for asters to position cleavage furrows [reviewed in Rappaport, 1996], though von Dassow et al. [2009] recently suggested that asters can communicate to the cortex without physical contact. How asters communicate with the cortex is addressed by other articles in this volume.

Aster–Aster Interactions

What happens when two neighboring asters grow to touch each other? This question was of great interest to Rappaport, since cleavage furrows are typically induced where and when microtubules growing from aster pairs meet at the cortex. Figure 5 shows three possibilities drawn from the literature, where the consequence of aster–aster interaction depends strongly on the system and cell cycle state. When asters grow from nearby centrosomes in pure tubulin, their microtubules simply interpenetrate (Fig. 5A) [see examples in Brinkley et al., 1981]. This is expected because the microtubules are too far apart in three dimensions to physically bump into each other. When two asters meet in mitotic *Xenopus* egg extract, they adhere, then move together and fuse [Fig. 5B, Gatlin et al., 2009]. Movement and fusion are driven by dynein in this system, presumably cross-bridging between two microtubules. When two asters meet during interphase in frog and fish embryos, their microtubules do not interpenetrate and the asters tend to move apart [Fig. 5C, Wühr et al., 2010]. Aster movement is again driven by dynein, but in this case the dynein is presumably anchored in the cytoplasm (discussed below), rather than to another microtubule, so it produces force in the opposite direction. An effect of cell cycle state on aster–aster interaction was also noted in echinoderm embryos using electron microscopy (EM) [Asnes and Schroeder, 1979]. Microtubules from the two asters of one spindle interpenetrated at the equator during metaphase. During anaphase–telophase there was no interpenetration at the equator, despite the fact that astral microtubules radiating away from the equator were longer on average. This classic observation suggests that some factor blocks aster interpenetration specifically during anaphase–telophase. More recent immunofluorescence images suggest some astral microtubule do cross the equator at anaphase–telophase (Fig. 4B), though this may be system-dependent.

Asters grow into each other in early embryos under different circumstances. Two asters grow out from the poles of each mitotic spindle at anaphase, and meet each other at the midplane of the cell (Figs. 1 and 2). We will call these "sister asters." The name traditional name for a pair of sister asters is the "amphiaster" [Wilson, 1925], from the Greek "amphi-" meaning "on both sides." The midplane between the asters has been called the "diastem" [Wilson, 1925] or "diastema" [e.g., Wakabayashi and Shinagawa, 2001], meaning space or gap between two structures. More recently, the term "telophase disc" was coined to describe the analogous location in somatic cells [Andreassen et al., 1991]. We will use the term "aster–aster interaction zone" for this midplane, to emphasize the process by which it forms. Non-sister asters meet in the zygote following polyspermic fertilization, when each sperm centrosome nucleates an aster, and after anaphase following polyspermy or cytokinesis failure, when asters growing from the poles of separate spindles meet. Examples of interactions between non-sister asters following polyspermic fertilization, before and after 1st mitosis, are shown in Fig. 6. Polyspermy is abnormal in *Xenopus* (and most frogs) and Zebrafish, but normal in many pleurodeles (newts and salamanders) [Fankhauser, 1948; Iwao, 1989], including axolotl (Fig. 6F, F′). In naturally polyspermic pleurodele zygotes, the excess male pronuclei and centrosomes that do not capture the single female pronucleus are destroyed by an unknown mechanism around prophase of 1st mitosis [Fankhauser, 1948]. This mechanism for eliminating excess nuclei and centrosomes is missing in frogs, so forced polyspermic fertilization leads to multiple spindles and multiple cleavage furrows (Fig. 6).

The most characteristic consequence of aster–aster interaction in interphase frog and fish embryos, seen for both

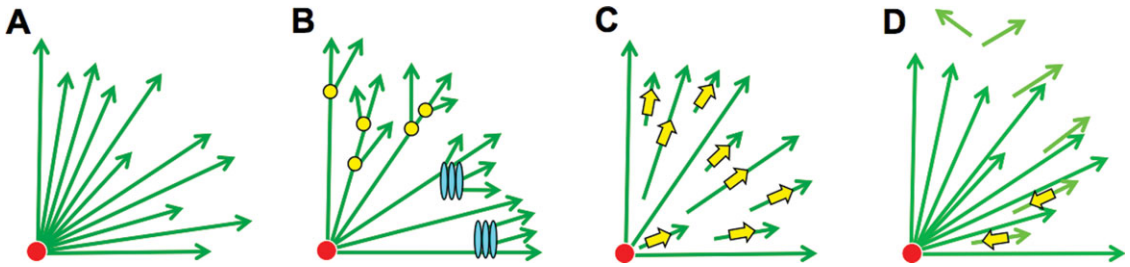

Fig. 3. Models for aster growth in large cells. A segment of the spherical aster is shown. Microtubule density at the aster periphery decreases with radius in model A. In the other models, microtubule density at the periphery can remain constant, or even increase, with radius. **A**: Conventional radial elongation. Minus ends are nucleated and retained at centrosomes (red circle) while plus ends (arrowheads) elongate. **B**: Nucleation away from the centrosome. As the aster grows, microtubules are nucleated from the side of preexisting microtubules (yellow circles), or from Golgi membranes (blue stacks). **C**: Release and outward transport. Minus ends are released from centrosomal nucleation sites, and microtubules slide outward (yellow arrows indicate sliding). **D**: Capture of non-astral microtubules. Microtubules are nucleated away from the aster, for example, at the cortex (pale green). As astral microtubules (dark green) grow out, they capture and orient the non-astral microtubules, and perhaps transport them inward (yellow arrows).

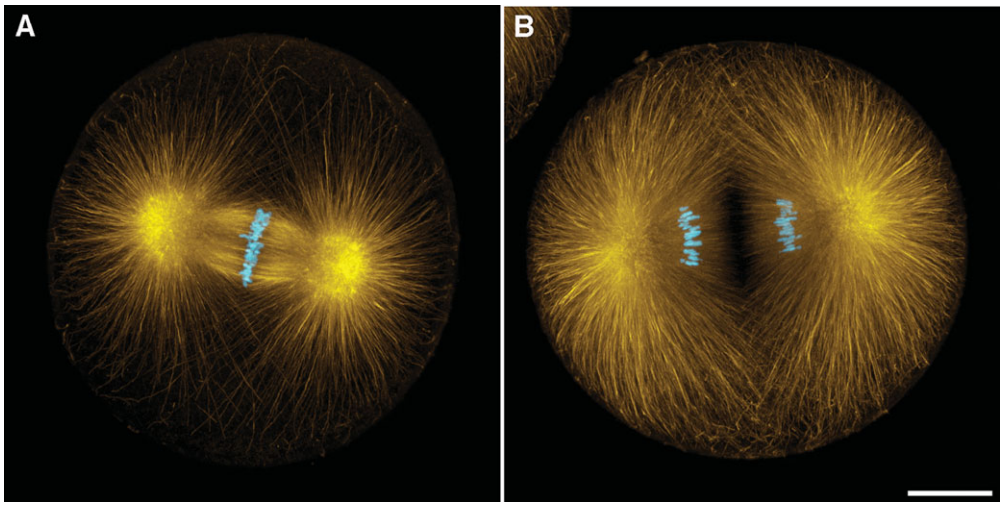

Fig. 4. Microtubules in zygotes of the nemertean worm Cerebratulus. Confocal images of fixed embryos kindly provided by George von Dassow, (Oregon Institute of Marine Biology). Images are projections of 61 sections spaced 0.3 μm apart. The microtubule distribution in metaphase (**A**) appears radial, and microtubule density decreases rapidly with radius. In late anaphase (**B**), it appears more bundled and bushy, and microtubule density decreases less with radius. The dark zone in the center in B is presumably caused by a steric block to antibody penetration. A similar block is present at the center of the anaphase midzone and telophase midbody in somatic cells, and may also be present at the center of the aster-aster interaction zone in frog and fish embryos.

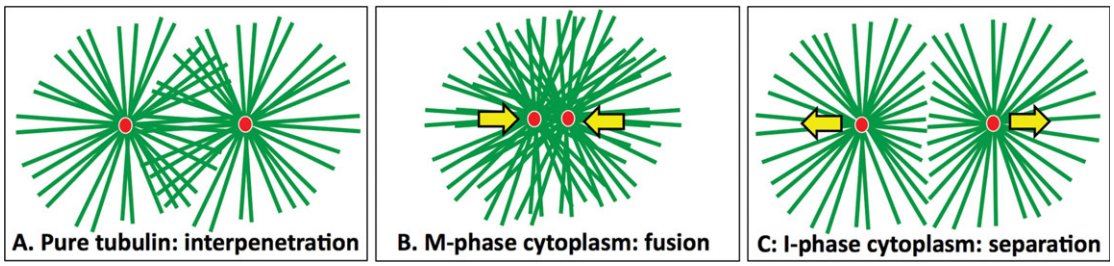

Fig. 5. Consequences of aster-aster interaction depend on the system. Possible branching nucleation is omitted for simplicity. **A**: In pure tubulin, plus ends simply grow past each other [Brinkley et al., 1981]. **B**: In M-phase extract prepared from unfertilized *Xenopus* eggs, asters (and spindles) that touch each other adhere, move together, and fuse. Movement is driven by dynein, which is thought to cross-bridge anti-parallel microtubules [Gatlin et al., 2009]. **C**: In interphase in early embryos, growing asters interact to generate a zone of anti-parallel overlap and low microtubule density at their mutual boundary. The asters then tend to move apart, pulled by cytoplasmic dynein anchored in bulk cytoplasm [Wühr et al., 2010], see text for details. A block to microtubule interpenetration during anaphase-telophase was also noted in a classic EM study in echinoderm embryos [Asnes and Schroeder, 1979].

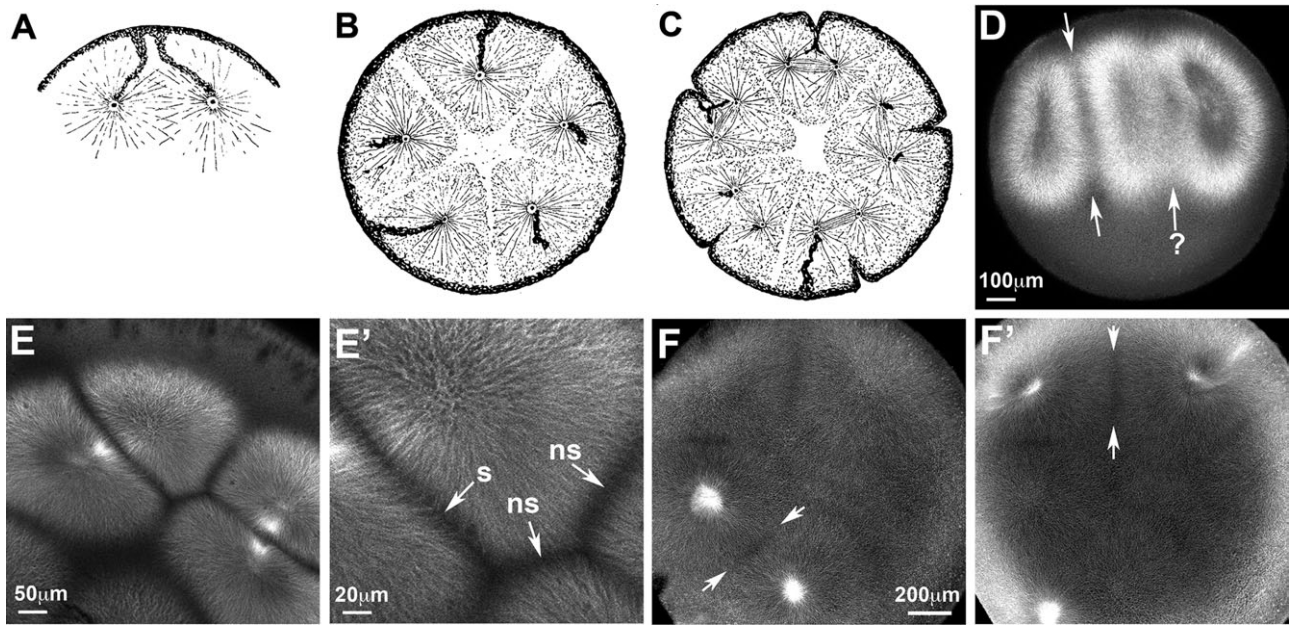

Fig. 6. Interaction of non-sister asters following polyspermic fertilization in amphibian embryos. A–C; Sequential stages from fertilization to 1st cleavage following forced polyspermy in the frog *R. fusca*. Images drawn from histological sections [Brachet, 1910]. **D–F** Tubulin staining in fixed embryos from *X. laevis* (D, E, E′) and the axolotl *Ambystoma mexicanum* (F, F′). A: Neighboring sperm asters tend to move apart as they center. B: Asters tend to space out regularly before 1st mitosis, dividing the cytoplasm into regularly spaced units. C: Cleavage furrows are induced between sister asters at 1st cleavage in *R. fusca*, while zones between non-sisters do not. The same is true in *X. laevis* [Render and Elinson, 1986; Wakabayashi and Shinagawa, 2001]. D. Forced trispermy in *X. laevis*, stage between B and C. Note an interaction zone of low microtubule density between two asters (white arrows). The arrow marked with a ? indicates an interaction where some microtubule interpenetration may have occurred. E, E′: Forced polyspermy in *Xenopus*, stage a little earlier than C, after anaphase of 1st mitosis but before furrow induction. Two pairs of sister asters can be recognized in E by the brighter bundles of microtubules at the center of the interaction zone where the metaphase spindle used to be. Note the sharply defined interaction zones between both sister and non-sister asters. E′ is a higher mag. view from E where (s) denotes interaction zones between sister asters, and (ns) between non-sister asters. F, F′: Natural polyspermy in *Ambystoma mexicanum*, stage similar to B. Two focal planes are shown. This zygote contains at least six sperm. The egg is enormous (~3 mm) which makes imaging difficult. Arrows denote likely aster–aster interaction zones as planes between asters where microtubule density is low.

sister (Figs. 1 and 2) and non-sister (Fig. 6) pairs, is that the two asters do not interpenetrate deeply. Rather, they interact and then seem to repel each other. Based on images from living and fixed embryos, recently supplemented by images from asters interacting in egg extract, we believe aster interpenetration is blocked by formation of a specialized interaction zone at the mutual boundary. This zone exhibits certain common morphological features: (i) aster–aster interaction zones tend to define sharp planes that conceptually divide the cytoplasm, (ii) they exhibit an apparently lower (but non-zero) density of microtubules relative to nearby parts of the aster, (iii) microtubules in the interaction zone may be organized in bundles, presumably antiparallel, that are aligned approximately normal to the plane defined by the zone (Fig. 2C′). These morphological aspects of interaction zones strongly suggest that they act as boundaries that inhibit aster expansion and limit microtubule length, and that interaction between antiparallel microtubules lie at their core. The apparently lower microtubule density in interaction zones could be wholly or partly an imaging artifact. Midbody microtubules tend to exclude antibody staining, presumably due to steric effects. Antibody exclusion is presumably responsible for the dark zone between separating chromatids in the sea urchin image in Fig. 4B, and could contribute to lowered signal in interaction zones seen by immunofluorescence in *Xenopus* (Fig. 1). Exclusion of the ensconsin-GFP probe very likely contributes to lower intensity in aster–aster interaction zones in fish (Fig. 2). However, lower microtubule density is also observed using directly labeled tubulin in egg extracts (Fig. 8) and Zebrafish embryos [Wühr et al., 2011], so we suspect at least part of the drop in tubulin signal in the interaction zone is real, and reflects lower microtubule density there.

Despite common features, there are reasons to suspect that not all aster–aster interaction zones are the same. Most notably, furrows are induced where the interaction zones between sister asters reach the cortex after 1st mitosis, and not where interaction zones between non-sisters reach the cortex, in the frogs *Rana fusca* and *X. laevis*, [Fig. 6C, Brachet, 1910; Render and Elinson, 1986; Wakabayashi and Shinagawa, 2001]. This is the opposite result from that Rappaport [1961] obtained in his celebrated toroidal cell experiment in echinoderm eggs, where

the interaction between non-sister asters from two different spindles efficiently induced furrows if they were sufficiently close together. Non-sister asters also generated furrows at their interaction zone in tissue culture cells [Savoian et al., 1999] and *C. elegans* embryos [Baruni et al., 2008]. It is unclear why non-sister asters fail to initiate furrows in frogs, and this system may be useful for discriminating interaction zone molecules that are, and are not, required for furrow induction.

What molecules are likely to mediate aster–aster interactions in early frog and fish embryos? To our knowledge, no molecule has been specifically localized to aster–aster interaction zones in frog or fish embryos, but one logical set of candidates are molecules that organize cytokinesis midzone complexes in smaller cells [reviewed in Glotzer, 2005; Eggert et al., 2006]. Midzones, also called "central spindles," are barrel-shaped assemblies composed of antiparallel microtubule bundles that form between separating chromosomes in anaphase. Later, in telophase, they mature into midbodies, and this maturation is accompanied by relocalization of the microtubule organizing proteins [Hu et al., 2012]. Midzones in small animal cells and interaction zones between sister asters in large embryo cells are functionally analogous, and share key features of (i) antiparallel microtubule overlap at their center, (ii) limited polymerization at plus ends in the overlap region, and (iii) assembly in a cytoplasm where Cdk1 activity recently dropped, but Aurora B and Plk1 kinases are still active. Phragmoplasts, antiparallel microtubule arrays that direct formation of a new cell wall during cytokines in higher plants, also share some or all of these attributes. These similarities suggest organization by similar molecules. Consistent with this possibility, the midzone in *C. elegans* zygotes, which is larger than a typical somatic midzone, though still much smaller than aster interaction zones in frogs and fish, is organized by essentially the same molecules as somatic midzones [Glotzer, 2005].

Midzones are organized by three conserved protein modules or complexes [Glotzer, 2005, Eggert et al., 2006]: (i) Aurora B kinase complex or "chromosome passenger complex" [Ruchaud et al., 2007], (ii) Kif4/PRC1, and (iii) Kif23/RAPGAP1. Kif23 is also called CHO1 and MKLP1, RAPGAP1 is also called MgcRacGap and Cyk4, and the complex between them is also called Centralspindlin. We currently hypothesize that overlap between antiparallel microtubules (in the appropriate cell cycle state) is the feature that allows plus ends at the periphery of the two asters to recognize each other, though alternative models discussed in Wühr et al. [2009] have not been ruled out. At least two of the conserved midzone-organizing proteins (PRC1 and Kif23) are known to mediate interactions between antiparallel microtubules [Nislow et al., 1992, Mishima et al., 2002, Mollinari et al., 2002, Subramanian et al., 2010], and are thus candidates to mediate recognition between the peripheries of two growing asters. Once formed, interaction zones must somehow inhibit aster growth and deep interpenetration by growing plus ends. A candidate for this function is Kif4, a kinesin with plus end directed motor activity that also inhibits plus ends polymerization in vitro [Bringmann et al., 2004] and in somatic midzones [Hu et al., 2011]. Kif4 can be targeted to antiparallel overlaps by interaction with PRC1 [Bieling et al., 2010]. It will be interesting to test which midzone proteins localize to sister and non-sister interaction zones in frog and fish embryos. Aurora B localized to antiparallel microtubule bundles close the cleavage furrow in Zebrafish, and was required for normal microtubule organization and furrowing, but was not clearly recruited to interaction zones [Yabe et al., 2009]. We expect aster–aster interaction zones will share important molecular and organizational mechanisms with somatic midzones, but that additional mechanisms may be required to adapt a conserved organizing principle-interaction between antiparallel microtubules coupled to local recruitment of polymerization inhibitors - to very large length scales.

Aster and Centrosome Positioning

How asters, and the centrosomes at their centers, position themselves within embryos was also of great interest to Rappaport. Aster movement in large embryo cells is driven mainly by cytoplasmic dynein pulling on microtubules [Gönczy et al., 1999; Grill and Hyman, 2005; Wühr et al., 2010; Kimura and Kimura, 2011]. Pushing forces can also contribute to aster centering, and may dominate in small cells [Tran et al., 2001; Howard, 2006], but pulling by dynein is thought to dominate in large cells. Aster movements can be broadly classified into those that tend to center centrosomes within the cell, and those that tend to move them away from the center. The canonical example of centering is migration of the sperm centrosome, and its associated pronucleus, to the center of the zygote [Wilson, 1925; Hamaguchi and Hiramoto, 1986]. The canonical example of decentering is movement of one spindle pole toward the posterior cortex during metaphase–anaphase in *C. elegans* zygotes [Hyman, 1989]. The mechanistic distinction may hinge on whether dynein pulls from bulk cytoplasm (centering), or from localized regions on the cortex (decentering). Complex cleavage patterns, such as spiral cleavage [Wilson, 1925], may depend on a complex interplay of centering and decentering movements. Here, we will focus on centering, which predominate in early *Xenopus* and Zebrafish cleavage divisions.

Hamaguchi and Hiramoto [1986] postulated that the sperm centrosome centers in the zygote due to length-dependent pulling forces on astral microtubules, combined with limitation of microtubule length by interaction with the cortex. Their model was based on elegant experiments

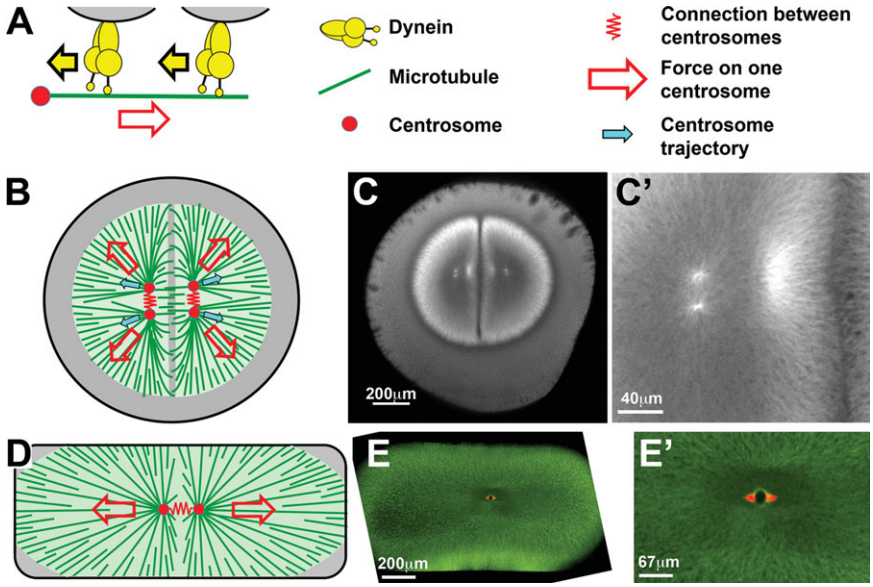

Fig. 7. Model for centrosome movement and orientation of the axis between centrosomes. A: Dynein in bulk cytoplasm, presumably anchored to organelles, generates a pulling force on centrosomes that increases with microtubule length [Hamaguchi and Hiramoto, 1986; Kimura and Kimura, 2011]. **B**: Orientation of centrosome pairs orthogonal to the aster–aster interaction zone. Sister asters are dome shaped at telophase due to the interaction zone. This results in microtubule lengths, and net force on each centrosome, as indicated. In response, centrosome pairs move away from the interaction zone, while the centrosomes within each pair separate and orient on an axis parallel to the interaction zone. The axis between the centrosomes will later become the axis of 2nd mitotic spindle [Wühr et al 2010]. **C**,C′: Example of centrosome separation within telophase asters following 1st mitosis in *Xenopus*. C′ is a high mag. view from C highlighting centrosomes. **D**: Model for forces on centrosomes in a compressed egg. Compression forces cleavage to orient across the short axis of the egg [Pflüger, 1884; Hertwig, 1893]. See Minc et al. [2011] for a mathematical model of this situation. E, E′: Recent repeat of Hertwig's classic egg compression experiment [Wühr, 2010]. This compressed egg was fixed in prophase and stained for tubulin (green) and γ-tubulin (red). The centrosome pair has already oriented along the long axis of the cell, presumably in response to compression of the sperm aster as indicated in D.

where local inactivation of colcemid with UV light was used to artificially control microtubule length distribution in echinoderm embryos. Recent mathematical models support the concept that asters center by pulling forces that increase with microtubule length [Kimura and Onami, 2005; Minc et al., 2011; Shinar et al., 2011]. Hiramoto et al suggested that motor-dependent forces that move vesicles and polystyrene beads toward centrosomes generate counter-forces that pull microtubules in the opposite direction [Hamaguchi et al., 1986; Hamaguchi and Hiramoto, 1986]. In *C. elegans*, dynein centers the sperm aster by pulling from anchor sites on endosomes and lysosomes, and a candidate anchoring protein has been identified [Kimura and Kimura, 2011], which confirms and extends Hiramoto's hypothesis.

We hypothesized that Hiramoto's basic idea, which is cartooned in Fig. 7A, can be extended to all centrosome movements in early frog and fish embryos simply by adding length-limitation by aster–aster interaction zones [Wühr et al., 2010]. Asters grow longer on the side away from the zone (Figs. 1, 2, and 6), so they should engage more dynein on that side, and thus move away from the zone. An example of centrosome movement away from an interaction zone is shown in the last panel in Fig. 2. In this model interaction zones and the cell cortex influence asters in the same way, by limiting their growth, and thus total microtubule length projecting in a particular direction. Accordingly, asters will naturally space out between each other and the cortex, as is seen for aster spacing in polyspermy [Brachet, 1910; Herlant, 1911] (Fig. 6). More complex models are possible, of course. For example, interaction zones might accumulate specific molecules that locally influence motor proteins.

Perhaps the most intriguing unexplained aspect of aster and centrosome movement is orthogonal orientation of successive cleavage planes in embryos with an orthoradial cleavage pattern [Wilson, 1925]. In *Xenopus*, the first three cleavage planes are approximately orthogonal to each other in three dimensions in most embryos. Figure 1D shows an example of the orthogonal relationship between the 1st cleavage plane (running north–south) and the presumptive 2nd planes which will run east–west, cutting through the interactions zones between sister asters in each blastomere. The first plane cuts through the sperm entrance point [Black and Vincent, 1988], and the first two planes both cut parallel to the animal-vegetal axis. Early Zebrafish blastomeres (which do not cleave completely) are confined to two dimensions, presumably

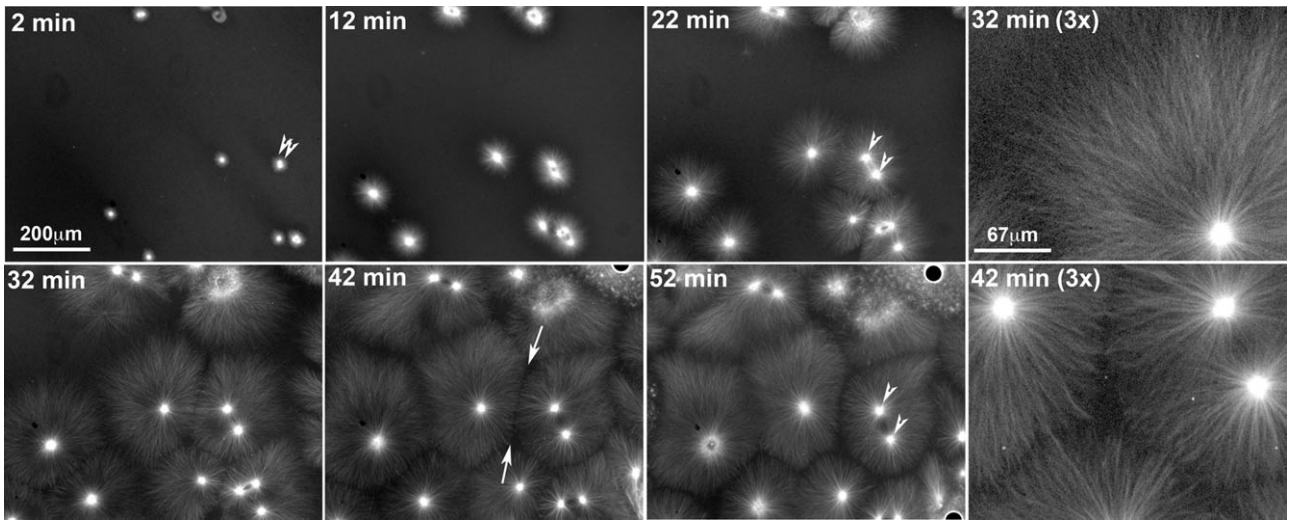

Fig. 8. Preliminary recapitulation of interphase aster growth and interaction in a cell free system. *Xenopus* egg mitotic extract [Desai, 1999] was mixed with fluorescent tubulin and artificial centrosomes [Tsai and Zheng, 2005], converted to interphase with Ca^{++}, spread between passivated coverslips and imaged by widefield fluorescence microscopy with a ×10 objective. Large asters grew with a bushy morphology at their peripheries (e.g., 32 min [×3]). When asters grew to touch each they generated interaction zones with locally low microtubule density (e.g., arrows at 42 min, shown at higher mag. in 42 min [×3]). These interaction zones blocked aster expansion and were stable for tens of minutes (compare 32, 52 min). When two artificial centrosomes were initially close together, they tended to initiate a single aster, and later split apart within that aster (e.g., the pair indicated by arrowheads at 2, 22, and 53 min). This splitting was reminiscent of centrosome separation within telophase asters in embryos (Fig. 6C).

because the yolk-free cytoplasm is laid down as a sheet in the oocyte. Successive cleavage planes are approximately orthogonal in two dimensions.

Although cleavage plane geometry is stereotyped in frog eggs, it is not rigidly prespecified. Changing the shape of the egg, or the distribution of yolk within it [Chung et al., 1994], can override intrinsic tendencies to cleave with a particular geometry. In a classic example, frog eggs squeezed into elongated shapes cleave normal to the imposed long axis [Pflüger, 1884; Hertwig, 1893], overriding the intrinsic tendency of the first cleavage furrow to bisect the sperm entrance point. Rappaport [1996] explored may variations of this kind of experiment in echinoderm eggs. The plasticity in cleavage plane geometry revealed by this kind of experiment suggests that the orthogonal orientation of successive planes is not a consequence of some hard-wired property of the system, such as the angle between mother and daughter centrioles, but is rather an emergent property that depends on aster shape and forces within asters.

Figure 7B presents a model for orthogonal orientation of successive cleavage planes based on Hiramoto-pulling (Fig. 7A) combined with microtubule length limitation by aster–aster interactions [Wühr et al., 2010]. Key to this model is our observations that the two centrosomes within each aster split apart as the dome-shaped aster grows during telophase (examples shown in Fig. 7C′ for frog and the last panel in Fig. 2 for fish). The next metaphase spindle will set up on the axis defined by centrosome splitting at this stage [Wühr et al., 2010]. We hypothesize that the dome shape of the aster causes asymmetries in microtubule lengths, and therefore in dynein pulling forces pulling on centrosomes. These pull the centrosome pair apart along the longest axis of the aster, which is parallel to the interaction zone (Fig. 7B). Some additional asymmetry is required to orient centrosomes relative the *z*-axis in Fig. 7B, equivalent to the animal-vegetal axis in the zygote. We do not understand this aspect, though we suspect it depends on the gradient of yolk in the *z*-axis. Figure 7D cartoons the equivalent model for orientation of the first cleavage plane by compression of the egg [Pflüger, 1884; Hertwig, 1893], along with images from a recent repeat of this experiment where we demonstrated that the axis between centrosomes is already orientated in prophase, implying the geometry of the compressed egg is sensed by the sperm aster before 1st mitosis [Wühr et al., 2010]. Minc et al. [2011] built a mathematical model of situations similar to Fig. 7D in sea urchin zygotes, and tested it by systematically deforming the egg into different shapes. The agreement they found between experiment and model is encouraging, but it is important to realize that Figs. 7B and 7D, Kimura and Onami [2005], Wühr et al. [2010] and Minc et al. [2011] all make untested assumptions about the spatial distribution of microtubules, and the forces acting on them. It is also notable that these models fail to predict or explain the wavy, somewhat disorganized appearance of individual microtubules and bundles at the aster periphery (evident in Fig. 2). It is not clear if pulling force-per-unit-length models are still valid if individual microtubules are shorter than the aster radius. Many questions remain as to how asters and centrosomes are positioned in early embryos.

Cell-Free Reconstitution of Interphase Aster Growth and Interaction

It will be difficult to elucidate the molecular and biophysical mechanisms involved in aster dynamics using whole, living embryos as the only experimental system, especially in *Xenopus* where the egg is opaque. The related problem of meiosis-II spindle assembly in *Xenopus* eggs was tackled using cell-free extracts that accurately recapitulated the assembly process and greatly facilitated imaging and perturbation experiments [Desai et al., 1999; Maresca and Heald, 2006]. *Xenopus* egg extract is essentially undiluted cytoplasm with abundant organelles and vigorous energy metabolism [Niethammer et al., 2008]. We recently modified this system to mimic polyspermic fertilization (Fig. 8). We observed rapid growth of large interphase asters and formation of aster–aster interaction zones when asters grew into each other (e.g., arrows in Fig. 8, 42 min). Aster morphology in this system recapitulated key aspects noted in embryos by immunofluorescence and live imaging, including "bushy" peripheries, locally low density of microtubules in interaction zones, and a tendency of closely spaced nucleating sites to split apart within single asters. This system should facilitate progress on molecular and biophysical mechanisms that underlie aster dynamics in large embryo cells.

Questions and Directions

In closing, we will highlight key questions from each section of this review where we need to uncover new molecular and biophysical mechanisms. (i) *Aster growth*: what is the mechanism for keeping microtubule density constant as aster radius expands? If microtubules nucleate away from the centrosome as we suspect, what is the mechanism? (ii) *Aster-aster interaction*: how do growing asters recognize each other when they touch, and how does this recognition lead to inhibition of aster growth? To what extent are interaction zones between sister and non-sister asters similar at the molecular level, and why do only the former induce furrows in frog zygotes at 1st mitosis? (iii) *Aster positioning*: can we find further experimental validation for the Hiramoto model for aster centering? How do centrosomes split apart within growing asters, and what determines the axis on which they separate?

Answering these questions will surely require interdisciplinary approaches that combine imaging, biochemistry, genetics, physical perturbation, force measurement, and computational modeling. Different biological systems have complementary advantages for these approaches, and we expect that *Xenopus* egg extract will prove particularly versatile. Vertebrate embryos with extremely large cells, where aster dynamics operate at a physical extreme, will help elucidate not only general principles of physical organization of cells, but also how these principles scale with cell size.

Acknowledgments

This work was supported by NIH GM39565. The authors thank Nikon Inc. for support of microscopy at the HMS Nikon Imaging Center and MBL. Work at MBL was supported by fellowships from the Evans Foundation, MBL Associates, and the Laura and Authur Colwin Summer Research Fund. They thank Sean Megason (HMS) and Angela DePace (HMS) for advice and time on their confocal microscopes. They thank Elly Tanaka (TU Dresden) and Mirjam Mayer (Whitehead Institute) for providing fixed axolotl zygotes. They also thank George von Dassow (Oregon Institute for Marine Biology) for providing unpublished data (Fig. 4) as well as stimulating discussion.

References

Ahmad FJ, Baas PW. 1995. Microtubules released from the neuronal centrosome are transported into the axon. J Cell Sci 108: 2761–2769.

Andreassen PR, Palmer DK, Wener MH, Margolis RL. 1991. Telophase disc: a new mammalian mitotic organelle that bisects telophase cells with a possible function in cytokinesis. J Cell Sci 99: 523–534.

Asnes CF, Schroeder TE. 1979. Cell cleavage. Ultrastructural evidence against equatorial stimulation by aster microtubules. Exp Cell Res 122:327–38.

Baruni JR, Munro EM, von Dassow G. 2008. Cytokinetic furrowing in toroidal, binucleate and anucleate cells in C. elegans embryos. J Cell Sci 121:306–316.

Becker BE, Gard DL. 2006. Visualization of the cytoskeleton in Xenopus oocytes and eggs by confocal immunofluorescence microscopy. Methods Mol Biol. 322:69–86.

Belmont LD, Hyman AA, Sawin KE, Mitchison TJ. 1990. Real-time visualization of cell cycle-dependent changes in microtubule dynamics in cytoplasmic extracts. Cell 62:579–589.

Bergen LG, Kuriyama R, Borisy GG. 1980. Polarity of microtubules nucleated by centrosomes and chromosomes of Chinese hamster ovary cells in vitro. J Cell Biol 84:151–159.

Bieling P, Telley IA, Surrey T. 2010. A minimal midzone protein module controls formation and length of antiparallel microtubule overlaps. Cell 142:420–432.

Black SD, Vincent JP. 1988. The first cleavage plane and the embryonic axis are determined by separate mechanisms in Xenopus laevis. II. Experimental dissociation by lateral compression of the egg. Dev Biol 128:65–71.

Blow JJ. 2001. Control of chromosomal DNA replication in the early *Xenopus* embryo. EMBO J 20:3293–3297

Brachet A. 1910. La polyspermie experimental comme moyen d'analyse de la fecondacion. Arch Entwicklungsmech Org 30: 261–303.

Bringmann H, Skiniotis G, Spilker A, Kandels-Lewis S, Vernos I, Surrey T. 2004. A kinesin-like motor inhibits microtubule dynamic instability. Science 303:1519–1522.

Brinkley BR. 1985. Microtubule organizing centers. Annu Rev Cell Biol 1:145–172.

Brinkley BR, Cox SM, Pepper DA, Wible L, Brenner SL, Pardue RL. 1981. Tubulin assembly sites and the organization of cytoplasmic microtubules in cultured mammalian cells. J Cell Biol 90: 554–562.

Burbank KS, Groen AC, Perlman ZE, Fisher DS, Mitchison TJ. 2006. A new method reveals microtubule minus ends throughout the meiotic spindle. J Cell Biol 175:369–375.

Chan RC, Forbes DI. 2006. In vitro study of nuclear assembly and nuclear import using Xenopus egg extracts. Methods Mol Biol 322: 289–300.

Chan J, Sambade A, Calder G, Lloyd C. 2009. Arabidopsis cortical microtubules are initiated along, as well as branching from, existing microtubules. Plant Cell 21:2298–2306.

Choi YK, Liu P, Sze SK, Dai C, Qi RZ. 2010. CDK5RAP2 stimulates microtubule nucleation by the gamma-tubulin ring complex. J Cell Biol 13;191(6):1089–1095.

Chung HM, Yokota H, Dent A, Malacinski GM, Neff AW. 1994. The location of the third cleavage plane of Xenopus embryos partitions morphogenetic information in animal quartets. Int J Dev Biol 38: 421–428

Decker M, Jaensch S, Pozniakovsky A, Zinke A, O'Connell KF, Zachariae W, Myers E, Hyman AA. 2011. Limiting amounts of centrosome material set centrosome size in C. elegans embryos. Curr Biol 21:1259–1267.

Desai A, Murray A, Mitchison TJ, Walczak CE. 1999. The use of Xenopus egg extracts to study mitotic spindle assembly and function in vitro. Methods Cell Biol 61:385–412.

Efimov A, Kharitonov A, Efimova N, Loncarek J, Miller PM, Andreyeva N, Gleeson P, Galjart N, Maia AR, McLeod IX, Yates JR, III, Maiato H, Khodjakov A, Akhmanova A, Kaverina I. 2007. Asymmetric CLASP-dependent nucleation of noncentrosomal microtubules at the trans-Golgi network. Dev Cell 12:917–930.

Eggert US, Mitchison TJ, Field CM. 2006. Animal cytokinesis: from parts list to mechanisms. Annu Rev Biochem 75:543–566.

Fankhauser G. 1948. The organization of the amphibian egg during fertilization and cleavage. Ann N Y Acad Sci 49(Art 5):684–708

Foe VE, von Dassow G. 2008. Stable and dynamic microtubules coordinately shape the myosin activation zone during cytokinetic furrow formation. J Cell Biol 183:457–470.

Gatlin JC, Matov A, Groen AC, Needleman DJ, Maresca TJ, Danuser G, Mitchison TJ, Salmon ED. 2009. Spindle fusion requires dynein-mediated sliding of oppositely oriented microtubules. Curr Biol 19:287–296.

Glotzer M. 2005. The molecular requirements for cytokinesis. Science 307:1735–1739.

Gönczy P, Pichler S, Kirkham M, Hyman AA. 1999 Cytoplasmic dynein is required for distinct aspects of MTOC positioning, including centrosome separation, in the one cell stage Caenorhabditis elegans embryo. J Cell Biol 147:135–150

Grill SW, Hyman AA. 2005. Spindle positioning by cortical pulling forces. Dev Cell 8:461–465.

Hamaguchi MS, Hiramoto Y. 1986. Analysis of the role of astral rays in pronuclear migration in sand dollar eggs by the colcemid-UV method. Dev Growth Differ 28:143–156

Hamaguchi MS, Hamaguchi Y, Hiramoto Y. 1986. Polystyrene beads move along astral rays in sand dollar eggs. Dev Growth Differ 28:461–470.

Herlant, M. 1911. Recherches sur les oeufs di-et-trispermiques de grenouille. Archs Biol 26:103–328.

Hertwig O. 1893. Ueber den Werth der ersten Furchungszellen fuer die Organbildung des Embryo. Experimentelle Studien am Frosch- und Tritonei. Arch mikr Anat xlii 662–807.

Howard J. 2006. Elastic and damping forces generated by confined arrays of dynamic microtubules. Phys Biol 3:54–66.

Hu CK, Coughlin M, Field CM, Mitchison TJ. 2011. KIF4 regulates midzone length during cytokinesis. Curr Biol 21:815–824.

Hu CK, Coughlin M, Mitchison TJ. 2012. Midbody assembly and its regulation during cytokinesis. Mol Biol Cell 23:1024–1034.

Hyman AA. 1989. Centrosome movement in the early divisions of Caenorhabditis elegans: a cortical site determining centrosome position. J Cell Biol 109:1185–1193.

Iwao Y. 1989. An electrically mediated block to polyspermy in the primitive urodele Hynobis nebulous and phylogenetic comparison with other amphibians. Dev Biol 134:438–445.

Kimura A, Onami S. 2005. Computer simulations and image processing reveal length-dependent pulling force as the primary mechanism for C. elegans male pronuclear migration. Dev Cell 8:765–775.

Kimura K, Kimura A. 2011. Intracellular organelles mediate cytoplasmic pulling force for centrosome centration in the Caenorhabditis elegans early embryo. Proc Natl Acad Sci USA 108(1):137–142.

Kirik A, Ehrhardt DW, Kirik V. 2012. TONNEAU2/FASS regulates the geometry of microtubule nucleation and cortical array organization in interphase Arabidopsis cells. Plant Cell 24:1158–1170.

Klymkowsky MW, Hanken J. 1991. Whole-mount staining of Xenopus and other vertebrates. Methods Cell Biol 36:419–441

Kollman JM, Merdes A, Mourey L, Agard DA. 2011. Microtubule nucleation by γ-tubulin complexes. Nat Rev Mol Cell Biol 2(11): 709–721

Lüders J, Stearns T. 2007. Microtubule-organizing centres: a re-evaluation. Nat Rev Mol Cell Biol 8:161–167.

Maresca TJ, Heald R. 2006. Methods for studying spindle assembly and chromosome condensation in Xenopus egg extracts. Methods Mol Biol 322:459–474.

Minc N, Burgess D, Chang F. 2011. Influence of cell geometry on division-plane positioning. Cell 144:414–426.

Mishima M, Kaitna S, Glotzer M. 2002. Central spindle assembly and cytokinesis require a kinesin-like protein/RhoGAP complex with microtubule bundling activity. Dev Cell 2:41–54.

Mollinari C, Kleman JP, Jiang W, Schoehn G, Hunter T, Margolis RL. 2002. PRC1 is a microtubule binding and bundling protein essential to maintain the mitotic spindle midzone. J Cell Biol 157: 1175–1186.

Morgan DO. 2006. The Cell Cycle. Principles of Control. Orby, Northants, UK: Oxford University Press.

Murata T, Sonobe S, Baskin TI, Hyodo S, Hasezawa S, Nagata T, Horio T, Hasebe M. 2005. Microtubule-dependent microtubule nucleation based on recruitment of gamma-tubulin in higher plants. Nat Cell Biol 7(10):961–968.

Niethammer P, Kronja I, Kandels-Lewis S, Rybina S, Bastiaens P, Karsenti E. 2007. Discrete states of a protein interaction network govern interphase and mitotic microtubule dynamics. PLoS Biol 5(2):e29.

Niethammer P, Kueh HY, Mitchison TJ. 2008. Spatial patterning of metabolism by mitochondria, oxygen, and energy sinks in a model cytoplasm. Curr Biol 18:586–591.

Nislow C, Lombillo VA, Kuriyama R, McIntosh JR. 1992. A plus-end-directed motor enzyme that moves antiparallel microtubules in vitro localizes to the interzone of mitotic spindles. Nature 359: 543–547.

Pflüger E. 1884. Ueber die Einwirkung der Schwerkraft und anderer Bedingungen auf die Richtung der Zelltheilung. Pflügers Archiv. 34:607–616.

Pollard TD, Borisy GG. 2003. Cellular motility driven by assembly and disassembly of actin filaments. Cell 112:453–465.

Rappaport R 1961 Experiments concerning the cleavage stimulus in Sand Dollar eggs. J Exp Zool 148:81–89.

Rappaport R. 1996. Cytokinesis in Animal Cells. UK: Cambridge University Press.

Render JA, Elinson RP. 1986. Axis determination in polyspermic Xenopus laevis eggs. Dev Biol 115:425–433.

Rivero S, Cardenas J, Bornens M, Rios RM. 2009. Microtubule nucleation at the cis-side of the Golgi apparatus requires AKAP450 and GM130. EMBO J 28:1016–1028.

Ruchaud S, Carmena M, Earnshaw WC. 2007. Chromosomal passengers: conducting cell division. Nat Rev Mol Cell Biol 8: 798–812.

Rusan NM, Tulu US, Fagerstrom C, Wadsworth P. 2002. Reorganization of the microtubule array in prophase/prometaphase requires cytoplasmic dynein-dependent microtubule transport. J Cell Biol 158:997–1003.

Samejima I, Lourenço PC, Snaith HA, Sawin KE. 2006. Fission yeast mto2p regulates microtubule nucleation by the centrosomin-related protein mto1p. Mol Biol Cell 16:3040–3051.

Savoian MS, Earnshaw WC, Khodjakov A, Rieder CL. 1999. Cleavage furrows formed between centrosomes lacking an intervening spindle and chromosome contain microtubule bundles, INCENP and CHO1, but not CENP-E. Mol Biol Cell 10:297–311.

Shinar T, Mana M, Piano F, Shelley MJ. 2011. A model of cytoplasmically driven microtubule-based motion in the single-celled Caenorhabditis elegans embryo. Proc Natl Acad Sci USA 108:10508–10513.

Srayko M, Kaya A, Stamford J, Hyman AA. 2005. Identification and characterization of factors required for microtubule growth and nucleation in the early C. elegans embryo. Dev Cell 9:223–236.

Strickland L, von Dassow G, Ellenberg J, Foe V, Lenart P, Burgess D. 2004. Light microscopy of echinoderm embryos. Methods Cell Biol 74:371–409.

Subramanian R, Wilson-Kubalek EM, Arthur CP, Bick MJ, Campbell EA, Darst SA, Milligan RA, Kapoor TM. 2010. Insights into antiparallel microtubule crosslinking by PRC1, a conserved nonmotor microtubule binding protein. Cell 142:433–443.

Tran PT, Marsh L, Doye V, Inoué S, Chang F. 2001. A mechanism for nuclear positioning in fission yeast based on microtubule pushing. J Cell Biol 153:397–411.

Tsai MY, Zheng Y. 2005. Aurora A kinase-coated beads function as microtubule-organizing centers and enhance RanGTP-induced spindle assembly. Curr Biol 15:2156–2163.

Uehara R, Nozawa RS, Tomioka A, Petry S, Vale RD, Obuse C, Goshima G. 2009. The augmin complex plays a critical role in spindle microtubule generation for mitotic progression and cytokinesis in human cells. Proc Natl Acad Sci USA 106:6998–7003.

Verde F, Dogterom M, Stelzer E, Karsenti E, Leibler S. 1992. Control of microtubule dynamics and length by cyclin A- and cyclin B-dependent kinases in Xenopus egg extracts. J Cell Biol 118: 1097–1108.

von Dassow G, Verbrugghe KJ, Miller AL, Sider JR, Bement WM. 2009. Action at a distance during cytokinesis. J Cell Biol 187:831–845.

Wakabayashi Y, Shinagawa A. 2001. Presence of a nucleus or nucleus-deriving factors is indispensable for the formation of the spindle, the diastema and the cleavage furrow in the blastomere of the Xenopus embryo. Dev Growth Differ 43:633–646.

Wilson EB. 1925. The Cell in Development and Heredity, 3rd ed. NY: McMillan.

Wühr M, Chen Y, Dumont S, Groen AC, Needleman DJ, Salic A, Mitchison TJ. 2008. Evidence for an upper limit to mitotic spindle length. Curr Biol 18:1256–1261.

Wühr M, Dumont S, Groen AC, Needleman DJ, Mitchison TJ. 2009. How does a millimeter-sized cell find its center? Cell Cycle 15;8(8):1115–1121.

Wühr M, Tan ES, Parker SK, Detrich HW, III, Mitchison TJ. 2010. A model for cleavage plane determination in early amphibian and fish embryos. Curr Biol 20:2040–2045.

Wühr M, Obholzer ND, Megason SG, Detrich HW, III, Mitchison TJ. 2011. Live imaging of the cytoskeleton in early cleavage-stage zebrafish embryos. Methods Cell Biol 101:1–18

Yabe T, Ge X, Lindeman R, Nair S, Runke G, Mullins MC, Pelegri F. 2009. The maternal-effect gene cellular island encodes aurora B kinase and is essential for furrow formation in the early zebrafish embryo. PLoS Genet 5(6):e1000518